Published in final edited form as:

Anal Bioanal Chem. 2015 May; 407(12): 3277-3283. doi:10.1007/s00216-015-8580-y.

Multi-color reflectance imaging of middle ear pathology in vivo

Tulio A. Valdez,

Department of Pediatric Otolaryngology, Connecticut Children's Medical Center, Hartford, CT 06106, USA

Nicolas Spegazzini,

G. R. Harrison Spectroscopy Laboratory, Massachusetts Institute of Technology, Cambridge, MA 02139, USA

Rishikesh Pandey,

G. R. Harrison Spectroscopy Laboratory, Massachusetts Institute of Technology, Cambridge, MA 02139, USA

Kaitlyn Longo,

Biodynamics Laboratory, University of Connecticut Health Center, Farmington, CT 06030, USA

Christopher Grindle,

Department of Pediatric Otolaryngology, Connecticut Children's Medical Center, Hartford, CT 06106, USA

Donald Peterson, and

Biodynamics Laboratory, University of Connecticut Health Center, Farmington, CT 06030, USA

Ishan Barman

Department of Mechanical Engineering and Oncology, Johns Hopkins University, Baltimore, MD 21218, USA

Tulio A. Valdez: tvaldez@connecticutchildrens.org; Ishan Barman: ibarman@jhu.edu

Abstract

Otoscopic examination using white-light illumination has remained virtually unchanged for well over a century. However, the limited contrast of white-light otoscopy constrains the ability to make accurate assessment of middle ear pathology and is subject to significant observer variability. Here, we employ a modified otoscope with multi-color imaging capabilities for superior characterization of the middle ear constituents in vivo and for enhanced diagnosis of acute otitis media and cholesteatoma. In this pilot study, five patients undergoing surgery for tympanostomy tube placement and congenital cholesteatoma excision were imaged using the custom-designed multi-color video-rate reflectance imaging system. We show that the multi-color imaging approach offers an increase in image contrast, thereby enabling clear visualization of the middle ear constituents, especially of the tympanic membrane vascularity. Differential absorption at the multiple wavelengths provides a measure of biochemical and morphological information,

Correspondence to: Tulio A. Valdez, tvaldez@connecticutchildrens.org; Ishan Barman, ibarman@jhu.edu. Electronic supplementary material The online version of this article (doi:10.1007/s00216-015-8580-y) contains supplementary material, which is available to authorized users.

and the rapid acquisition and analysis of these images aids in objective evaluation of the middle ear pathology. Our pilot study shows the potential of using label-free narrow-band reflectance imaging to differentiate middle ear pathological conditions from normal middle ear. This technique can aid in obtaining objective and reproducible diagnoses as well as provide assistance in guiding excisional procedures.

Keywords

Otoscopy; Acute otitis media; Reflectance; Autofluorescence; Imaging; Medical device

Introduction

Otoscopic diagnosis of middle ear conditions is largely dependent on a physician's ability to identify visual patterns in order to provide the adequate interpretation of a disease process. Although this method is of substantive clinical value, it hides a plethora of pathologic and physiologic changes that could have important therapeutic implications. Diagnosis of commonly observed (e.g., middle ear infection) as well as rare middle ear conditions (e.g., proliferative keratinized lesions) remains challenging in the clinical setting and suffers from significant observer variability. The accuracy of physician diagnosis with currently available methods has been shown to be lacking [1], with accurate diagnosis rates for otitis media ranging between 40 and 80 % [2–4] depending on the specific setting, age of the patient [2], and physician training [5].

Indeed, examinations in most physician practices still rely extensively on the white-light reflection, utilizing a standard otoscope—a device that has undergone hardly any modifications in modern times. This device is used by both primary care physicians and otolaryngologists for evaluation of otologic disease, ranging from common diagnoses such as otitis media (OM) to more complex and destructive disease processes such as cholesteatomas. Although a number of visual cues from the otoscopic evaluation can be utilized to predict middle ear pathology, decision analysis for a treatment strategy based on such factors is complicated.

Hence, there remains an unmet need for both diagnostic methods that quantify the myriad changes in disease to allow better prediction and reliable screening methods that can identify the disease presence for further tests. In this context, developing a diagnostic method that would provide objective molecular biomarker information of middle ear conditions and enhance subtle differences between different pathophysiological conditions would considerably alleviate the current problems associated with misdiagnosis.

A convenient and facile route to improve the diagnostic standards beyond that available with standard white light is by tuning illumination and detection conditions of otoscopic examination. Tissue illumination with specific wavelength light has been utilized in several diagnostic methods [6] including Wood's lamp, dermatologic autofluorescence [7], and endoscopic narrow-band imaging [8] (where the tissue is illuminated using a 10–20-nm wavelength band and the reflected light is recorded on a detector). Reflectance imaging is of particular interest as it can detect local changes in scattering and absorption of tissue

including changes in vascular density without substantially increasing system complexity and instrumentation costs.

However, the feasibility of narrow-band reflectance imaging for different pathophysiological conditions of the middle ear has not been assessed thus far. In this report, we adopt this approach and specialize it for use in conjunction with a minimally modified otoscope. We further show that the use of multiple wavelengths is advantageous for real-time diagnosis as the ability to combine wavelengths provides improved contrast. The results of our pilot study in human subjects with acute otitis media and cholesteatoma are reported to underline the potential of such an observer-invariant optical imaging approach as an adjunct to standard diagnosis.

Materials and methods

Instrument

The multi-wavelength narrow-band reflectance imaging video otoscope was designed as an add-on attachment to the standard Welch Allyn 3.5v MacroView Otoscope. The prototype of the reflectance video otoscope is presented in Fig. 1. The excitation source consists of two high-power light-emitting diodes (LEDs) in the visible (LZ4-00MD00, Mouser Electronics, USA) and UV (LZ1-000A00, Mouser Electronics, USA) regions, respectively. The visible source consists of four LEDs of different wavelengths, i.e., blue (455 nm), green (523 nm), red (625 nm), and the conventional broad-spectrum white light that can be operated individually or in combination. The UV source consists of a single LED, which emits in the 400–405-nm range. A base was specially designed and fabricated to align the detector, the filter wheel, the optical insert, and the Welch Allyn otoscope head on an optical axis. The filter wheel comprises three 1 -diameter filter slots, where one of the compartments was left empty to enable a traditional white-light-based otoscopic examination. While not used extensively in the present narrow-band reflectance imaging study, the filter wheel allows for facile incorporation of additional imaging modalities such as autofluorescence. Images were recorded on a CMOS camera (DCC1645C, 1280×1024 pixels, Thorlabs Inc.) mounted on the otoscope frame with the user-defined capability of recording either single-shot images or videos at up to 25 frames per second. Images were captured in JPEG or BMP and video recordings were in AVI format.

Data collection

The study was approved by the institutional review board at Connecticut Children's Medical Center. Inclusion of patients in this pilot study was limited to those undergoing an otologic surgical procedure under general anesthesia. The procedures included placement of bilateral myringotomy tubes as well as removal of congenital cholesteatomas. Contralateral normal ears were used as our control.

After initial visual inspection in each case, cerumen was removed to obtain an optimal view of the tympanic membrane. Our adapted otoscope using either a 2.5-mm or a 4-mm speculum was inserted into the external auditory canal until the physician (T.V.) was able to adequately identify and obtain a focused image of the tympanic membrane using white light.

Subsequent to identification of the normal anatomic landmarks of the tympanic membrane, multi-color narrow-band reflectance imaging was undertaken.

Data analysis

Spatial intensity maps and contrast enhancement were pursued in the MATLAB 8.3 environment (The MathWorks Inc.). In particular, we used the contrast-limited adaptive histogram equalization (CLAHE) algorithm that operates on small data regions (tiles) as opposed to conventional histogram equalization, which handles entire images. The contrast of each tile is improved so that the histogram of each output region approximately matches the specified histogram. In addition, the contrast enhancement can be limited in order to avoid amplifying the noise that may be present in the image. Here, contrast images were computed and used to objectively evaluate both normal and pathological ear conditions. Moreover, to quantify the difference in contrast between the white-light and multi-color reflectance images, histograms and corresponding cumulative distribution functions were constructed. The acquired images were also segmented into equally sized rectangular tiles to determine the contrast values for each piece by computing the ratio of the difference to the sum of the maximum and minimum intensity values. An average contrast value was then calculated for the entire image.

Results

Using the modified otoscope, images were obtained of the normal tympanic membrane, cholesteatoma, and acute otitis media using three individual wavelengths and one combination of two wavelengths, in addition to standard white-light imaging. The areas to be imaged were chosen by the physician and included areas that had previously been identified as abnormal on gross otoscopic examination. In this preliminary study, intraoperative imaging was performed on five patients, two of whom had congenital cholesteatomas while the three other patients were diagnosed with acute otitis media at the time of tympanostomy tube placement.

As seen in a representative image of a normal middle ear (Fig. 2A), standard white-light otoscopy offers adequate detailing of the tympanic membrane anatomy and vasculature. It also affords reasonable transtympanic illumination of the promontory, due to the translucent characteristics of the tympanic membrane. However, by simultaneously illuminating the same specimen with white-light and the 455-nm (blue) LED source, we observe a clear enhancement in the vasculature contrast and better detailing of the tympanic membrane especially the pars flaccida (Fig. 2B). Comparison of the corresponding CLAHE-derived intensity maps also underscores the better definition of the pars flaccida in the case with respect to white-light illumination alone. (Note that the histogram equalization process slightly masks the improvement in vasculature contrast using concomitant white-light and 455 nm illumination.) Critically, the recognizable features under white-light inspection are still maintained here, thereby aiding image interpretation by the physician.

Panels C–E of Fig. 2 show the single-wavelength images obtained using 625 nm (red), 455 nm (blue), and 523 nm (green) illumination, respectively. The image obtained using the red LED source (Fig. 2C) shows deep optical penetration, decent resolution of the promontory,

and crisp definition of the malleus, as also highlighted in the corresponding intensity map. The larger penetration depth expectedly stems from the relative lack of endogenous absorbers in this wavelength region. However, this image also exhibits poor characterization of the tympanic membrane and the vasculature. In contrast, Fig. 2D shows good definition of the tympanic membrane and the vasculature (because of substantive hemoglobin absorption in this region) but inferior determination of the malleus. The image obtained using the green source (Fig. 2E) is comparable to that acquired using the blue source with a slightly better detailing of the blood vessels. Significantly, when both the blue and green sources are employed in conjunction, the resultant image (Fig. 2F) reveals much better contrast of the vasculature and enhanced outline of the malleus than either panel C or D of Fig. 2. This suggests that a multi-wavelength reflectance imaging system serves as a better probe for selectively highlighting the various components of the middle ear physiology in a biochemically complex milieu. While the precise molecular sources of the reflectance data cannot be elucidated without a comprehensive spectral analysis, the combined wavelength images provide a measure of morphological and biochemical information that is unattainable in current practice.

In our two congenital cholesteatoma patients, an increased area of intensity is observed in the region of the lesion compared to the rest of the tympanic membrane and middle ear. In particular, we can view the definition of cholesteatoma in the posterior superior quadrant in Fig. 3 with well-delineated features of vascularity in the surrounding tympanic membrane. The increase in vasculature in the immediate vicinity of the congenital cholesteatoma is much more evident when both the blue and green sources are used simultaneously (Fig. 3B) as opposed to standard white-light imaging (Fig. 3A) or when either of the sources is used alone (data not shown here). On the other hand, the 625 nm illumination image in Fig. 3C enables superior detailing of the extension of the lesion. This allows better segmentation between the lateral process of the malleus and the lesion, which is substantially more difficult to achieve from direct observation of either panel A or B of Fig. 3. A comparison of the histograms for Fig. 3A, B also shows the higher tonal range in the latter case (see Electronic Supplementary Material (ESM) Fig. S1, where Fig. S1 (A) and S1 (B) provide the histograms and cumulative intensity distribution functions for panels A and B of Fig. 3, respectively). The average contrast values were calculated to be 0.75 and 0.81 for the whitelight image and the blue-green images, respectively, indicating a 6 % improvement in image contrast.

For the acute otitis media cases, the white-light images show the typical bulging tympanic membrane with purulent material behind it and increased vasculature. A representative white-light image of a patient with acute otitis media is given in Fig. 4A. Figure 4B is recorded with 455 nm illumination, which shows superior contrast as compared with white-light image (Fig. 4A). Figure 4C shows the corresponding image acquired using 523 nm green illumination, and while generally comparable to Fig. 4B, it offers clearer evidence of pus formation that is not easily perceived by using the blue LED source alone. This facet is further enhanced in the image obtained using simultaneous 455 and 523 nm illumination (Fig. 4D). The histograms for Fig. 4A, D also reveal the higher spread in intensity values corresponding to better contrast on simultaneous illumination with blue and green light sources in the latter case (see ESM Fig. S2, where Fig. S2 (A) and S2 (B) are the histograms

and cumulative intensity distribution functions for panels A and D of Fig. 4, respectively). We determined the mean contrast values to be 0.62 and 0.71 for the white-light image and the blue-green images, respectively, representing a 15 % improvement in image contrast.

Discussion

Standard otoscopic examination entails subjective visual interpretation by the physician based on white light reflecting off the tympanic membrane and the promontory, with additional input of the movement of the tympanic membrane via pneumatic otoscopy. The ability to make an adequate clinical diagnosis for middle ear conditions is, thus, largely dependent on the physician's experience and skill at recognizing morphological patterns under classical white-light illumination—and is intrinsically limited by the subjective nature of the assessment. In some conditions such as acute otitis media (AOM), establishing a diagnosis can be even more difficult due to the unspecific nature of the symptoms [9] and the limitations brought by an often challenging examination in an uncooperative patient population.

Spectroscopic imaging, combining the molecular basis of spectroscopy with real-time imaging capabilities, represents a new approach to move beyond obvious visual cues into utilizing the untapped biochemical information content. The ability to routinely define various tissue constituents and pathologies without human reliance would open an exciting world of objective analyses to understand biochemically disease onset and progression and to morphometrically investigate tissue structural response. In this context, the current study represents an exploratory effort to demonstrate how otoscopic examination of diverse pathologic conditions of the middle ear can be enhanced by utilization of different wavelengths. The modified otoscope utilizes a multi-color narrow-band reflectance imaging approach that exploits the changes in tissue absorption and scattering brought about by pathologic changes including the thickening and opacifying of the tympanic membrane, increasing of blood flow in hyperemia, and altering of normal anatomic contours and structures.

Our findings here illustrate the increased absorption in the blue and green regions of the spectrum in areas of high vascularity. Therefore, combining these two illumination sources or blue with white light offered much better detailing of the blood vessels, an important hallmark in evaluating a number of middle ear pathological conditions, than would be otherwise possible through classical otoscopic examination. Importantly, the multi-color narrow-band reflectance imaging can be performed in real time and at video rate, if so desired. Additionally, use of the red LED source enables deeper visualization due to the lower absorption at the wavelength, which is highly desirable to assess the pus accumulation in otitis media. Our study also reveals that use of the multi-color approach provides improved demarcation of critical morphological structures including the malleus, promontory, and the cholesteatoma lesion itself.

Furthermore, our ability to convert and analyze these images as spatial intensity maps in real time paves the way for objective assessment of the studied conditions. The CLAHE-derived images obtained in our study can be employed in supervised as well as unsupervised

segmentation frameworks to develop diagnostic algorithms that can indicate changes in function of the complex tissue structures without human intervention. It is in this context that we view the maximum utility of our approach, i.e., in reducing intra-observer variability prevalent in white-light otoscopic examination. Subjective assessments inferred manually are replaced, in this paradigm, by quantitative recognition permitting high-throughput, observer-invariant evaluation. The challenge in designing such algorithms is to ensure that the data analysis is rapid and robust (with respect to stochastic variance) and results in information that is statistically valid and readily interpretable by the physician.

Finally, it is worth noting that since no single combination can be said to highlight each diagnostically pertinent feature, we envision that investigation of a particular pathologic condition is likely to necessitate prior optimization of the set of illumination wavelengths best suited for its characterization. The advantage of our approach is that such a transition between the illumination wavelengths can be readily performed by digital control and does not require re-design or reassembly of a new customized device.

Conclusion

In this report, we have designed a modified otoscope that rapidly captures narrow-band reflectance image sequences, which potentially provides superior, observer-invariant assessment of middle ear pathology. The functionality of the multi-color narrow-band reflectance imaging approach is based on the underlying variances in absorption, scattering, and depth of penetration of different pathophysiological conditions arising from the intrinsic differences in chemical composition and morphology. To the best of our knowledge, this study constitutes the first attempt at simultaneously combining multiple illumination sources to provide additional morphological and biochemical detailing. We demonstrate the efficacy of this device in a pilot study of five patients with acute otitis media and congenital cholesteatoma. For both pathologic conditions, substantive improvement of visualization capability of critical diagnostic features is noted using the proposed approach. Increasing contrast between adjacent structures and targeting specific features of disease and inflammation such as hypervascularity can not only assist the physician at the time of making a diagnostic determination but also provide real-time guidance of surgical procedures.

While the studies performed here show the initial feasibility of this approach for middle ear application, significant work is needed to establish its true diagnostic benefit in larger-scale preclinical studies encompassing more diverse pathological conditions. Furthermore, we recognize that certain intrinsic limitations of otoscopic examination, such as the presence of cerumen and difficulty of evaluation in a crying toddler, also manifest themselves in the proposed modality. Also, narrow-band reflectance imaging may not provide adequate detection specificity to diagnose and differentiate more complex conditions, e.g., myringosclerosis from cholesteatoma.

Supplementary Material

Refer to Web version on PubMed Central for supplementary material.

Acknowledgments

This research was supported by the Connecticut Institute for Clinical and Translational Science (CICATS) and the JHU Whiting School of Engineering Startup Funds.

References

- 1. Blomgren K, Pitkaranta A. Int J Pediatr Otorhinolaryngol. 2005; 69:295-299. [PubMed: 15733586]
- 2. Jensen PM, Lous J. Fam Pract. 1999; 16:262–268. [PubMed: 10439980]
- 3. Pichichero ME, Casey JR. Pediatr Infect Dis J. 2008; 27:958–962. [PubMed: 18845985]
- 4. Takata GS, Chan LS, Morphew T, Mangione-Smith R, Morton SC, Shekelle P. Pediatrics. 2003; 112:1379–1387. [PubMed: 14654613]
- 5. Pichichero ME, Poole MD. Int J Pediatr Otorhinolaryngol. 2005; 69:361–366. [PubMed: 15733595]
- Roblyer D, Richards-Kortum R, Sokolov K, El-Naggar AK, Williams MD, Kurachi C, Gillenwater AM. J Biomed Opt. 2008; 13:024019. [PubMed: 18465982]
- 7. Ponka D, Baddar F. Can Fam Physician. 2012; 58:976. [PubMed: 22972730]
- 8. Tjon Pian Gi RE, Halmos GB, van Hemel BM, van den Heuvel ER, van der Laan BF, Plaat BE, Dikkers FG. Laryngoscope. 2012; 122:1826–1830. [PubMed: 22566012]
- 9. Niemel M, Uhari M, Jounio-Ervasti K, Luotonen J, Alho OP, Vierimaa E. Pediatr Infect Dis J. 1994; 13:765–768. [PubMed: 7808842]



Fig. 1. Photograph of the modified otoscope prototype with sequential white-light examination and narrow-band reflectance imaging capabilities. This prototype system was used in the human subject pilot study to evaluate the potential of the multi-wavelength reflectance imaging approach in evaluating middle ear pathological conditions

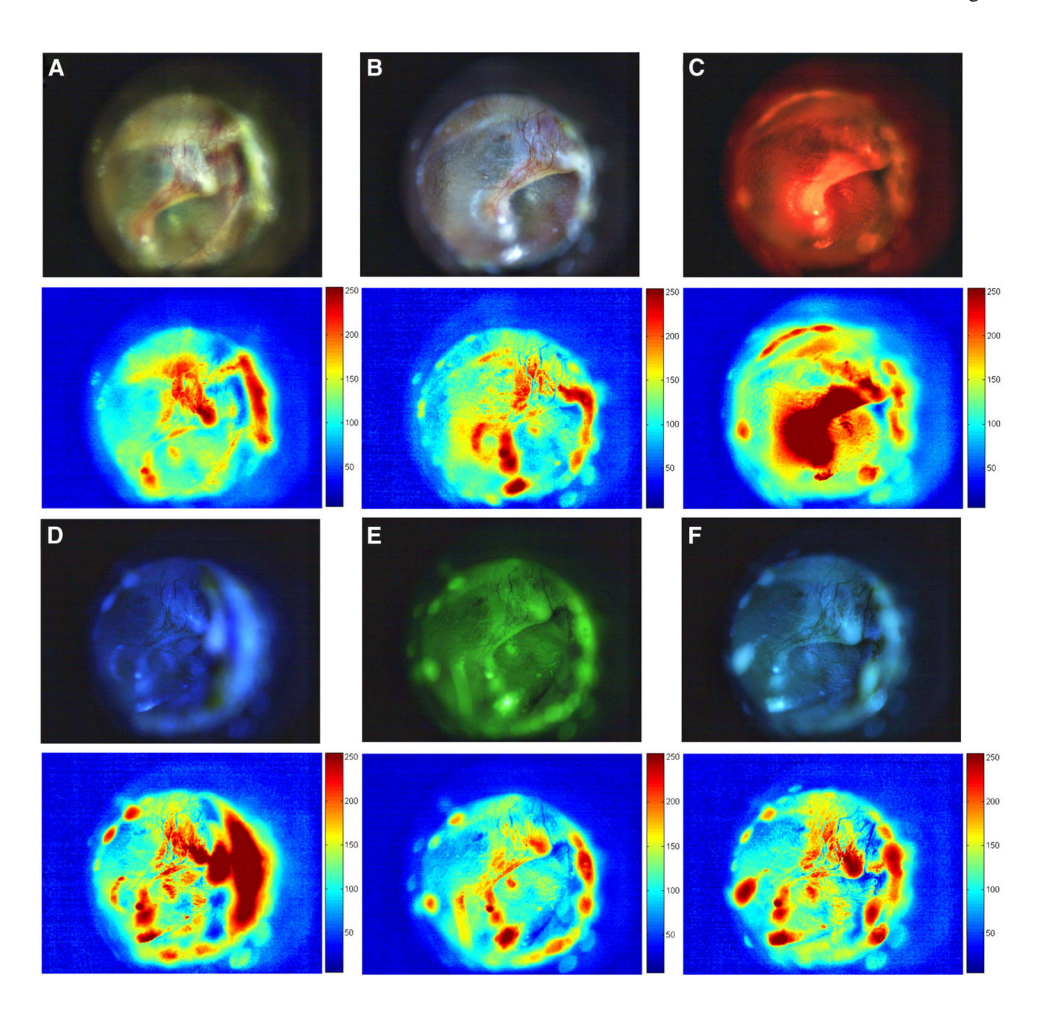


Fig. 2.

Images of normal tympanic membrane captured with **A** standard white-light illumination; **B** simultaneous white and blue light (455 nm) illumination; **C** red light (625 nm) illumination; **D** blue light illumination; **E** green light (523 nm) illumination; and **F** simultaneous blue and green light illumination. The corresponding CLAHE-derived spatial intensity maps are also provided to quantitatively assess the visualization possibilities under different illumination conditions. Specifically, comparison of **A** and **B** as well as **A** and **F** offers evidence of increase in contrast of vascularity on multi-color imaging compared to standard white-light otoscopy in the area of the malleus in a normal tympanic membrane. While in a normal tympanic membrane the vascularity plays no diagnostic role, in conditions such as acute otitis media and cholesteatoma, vascularity represents a critical diagnostic marker

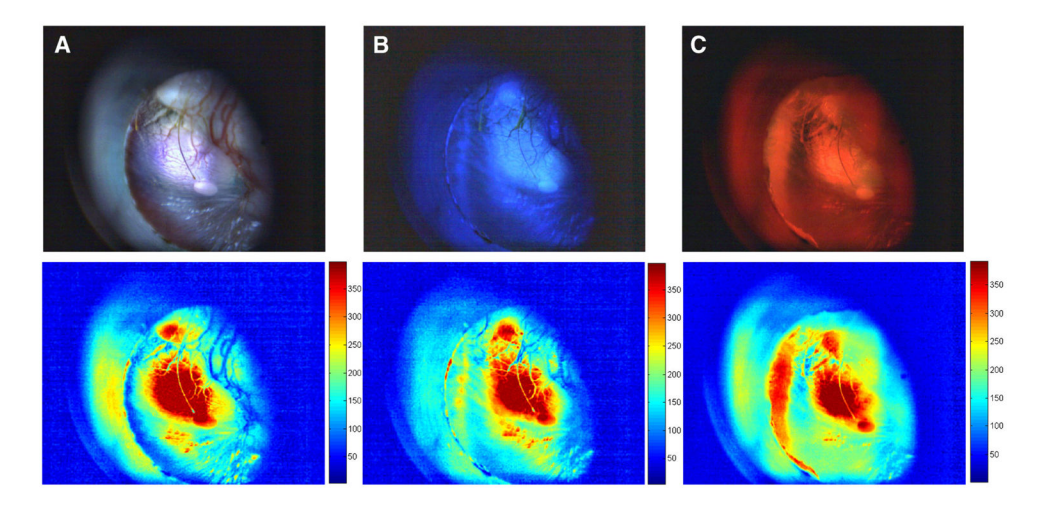


Fig. 3.
Representative images obtained from a patient with congenital cholesteatoma. The images were captured using **A** standard white-light illumination; **B** simultaneous blue light (455 nm) and green light (523 nm) illumination; and **C** red light (625 nm) illumination. In the *blue-green image*, the vasculature is enhanced that helps in diagnosis of proliferative lesions such as cholesteatoma. Additionally, the *red image* offers a sharper delineation of the lesion compared to the other images that can aid in preoperative planning

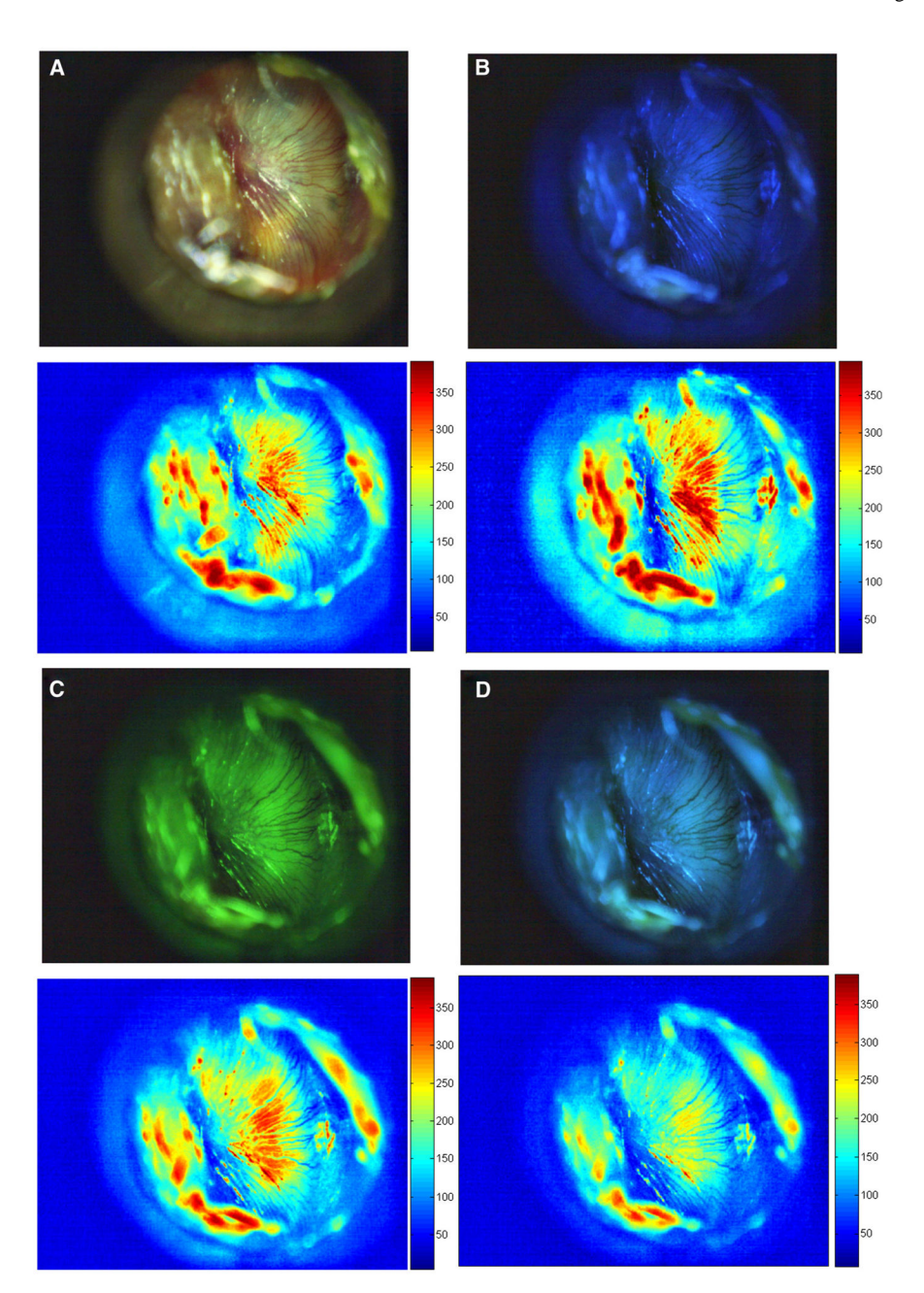


Fig. 4.
Representative images acquired from a patient's middle ear exhibiting acute otitis media.
The images were recorded using **A** standard white-light illumination; **B** blue light illumination; **C** green light (523 nm) illumination; and **D** simultaneous blue and green light illumination. Evidently, the *green* and *blue-green images* show increased contrast of the purulent material behind the tympanic membrane, which can be difficult to visualize on the white-light images